



## Eco-Friendly Electrical Insulating and Economic Styrene Butadiene Rubber Composites Reinforced With Porcelain Tiles Polishing Waste



CrossMark

Emad S. Shafik<sup>a\*</sup>, Nadia F. Youssef<sup>b</sup>

<sup>a</sup>Polymers and Pigments Department, National Research Centre (NRC), Dokki, Giza, Egypt

<sup>b</sup>Raw Building Materials Technology and Processing Research Institute, Housing and Building National Research Centre (HBRC), Dokki, Giza, Egypt

### Abstract

The ceramic construction industry is one of the most important over growing Egyptian industries. It satisfies local needs for the national ambitious housing projects other than exportation to many countries worldwide. As a result, it produces enormous amounts of solid wastes that harm environment other than economic loss. In this study, porcelain tiles polishing waste (PTW) is characterized using X-ray fluorescence (XRF), X-ray diffractometry (XRD) and particle size distribution. Therefore, the possibility of replacement of commercial kaolin with this fired waste as reinforced filler for styrene butadiene rubber (SBR) was assessed.

The rheological, physico-mechanical and electrical properties and thermal aging resistance for SBR composites were evaluated, in addition to evaluating the swelling properties and crosslinking density for prepared composites. The thermal stability of the composites was also evaluated using thermogravimetric analysis (TGA). The change in phase morphology using a scanning electron microscope was detected. The results showed that tensile strength, hardness shore A, and crosslinking density of SBR composites increased with increasing the waste weight ratio. In contrast, the elongation at break and the equilibrium swelling ratios decreased with increasing the waste weight ratio. Furthermore, the vulcanized sample containing 100% PTW waste shows higher retained tensile strength values than that containing 100% commercial kaolin, with increasing aging time. Finally it can be concluded that this waste can replace the commercial kaolin with observed improvement of mechanical, thermal and electrical insulation properties.

Keywords: electrical insulating; styrene butadiene rubber; composites; porcelain tiles polishing waste; ceramic floor tiles

### 1. Introduction

The fabrication of novel rubber composites is an exciting field of industrial research. The rubber composites produced in the industrial sector today should satisfy market requirements. So, researchers are working with rubber compounds and raw materials manufacturers to utilize wastes and to create novel techniques and rubber formulations [1, 2]. For example, styrene Butadiene Rubber (SBR) is widely used in a variety of industrial requests, including wire and cable protection, glues, toys made from rubber, molded rubber gains, shoe soles, pharmaceutical, surgical, and hygienic products [3,4].

The automotive industry used it for silent blocks and tires. Fillers, which are often added to the rubber matrix to advance the rubber's physical and mechanical qualities and ease the processing of raw materials broaden its applications. [5].

To enhance rubber composites processing and mechanical characteristics, fillers are frequently incorporated into the rubber matrix. Depending on the application area, fillers are divided into two major types: reinforcing and non-reinforcing. While non-reinforcing fillers are used to reduce the production costs which was done by increasing the end mass and

\*Corresponding author e-mail: emad.chemist@yahoo.com. (Emad S. Shafik)

Received date 2023-03-30; revised date 2023-05-07; accepted date 2023-05-25

DOI: 10.21608/EJCHEM.2023.203158.7798

©2023 National Information and Documentation Center (NIDOC)

volume of rubber products, reinforcing fillers are typically utilized to be mechanically enhanced [6]. Kaolin has been used in various consumer products, including rubber, paper, coatings, paper filling, paints, plastics, and similar materials, due to its desired properties, like being chemically inert and having low heat and electricity conductivity. In addition, since kaolin has strengthening and stiffness properties, it is employed by companies that produce rubber [7-9].

Numerous studies have documented the creation of innovative rubber and plastic end products based on various manufacturing or agricultural wastes, including red brick waste [10], recovered carbon black from waste [11], biochar from agricultural waste [12] and sunflower seed cake [13]. The attention of various researchers to dielectric materials with good dielectric performance has increased [14–16]. This was true for dielectric materials made of polymers, which have other benefits, including a small elastic module and ease of use other than energy storage applications [17–19]. Furthermore, blending fillers into the polymeric matrix to create filler/polymer complexes, some of them are called sandwich, is the most efficient way to syndicate the benefits of high dielectric constant and low dielectric loss matrix [20–22].

Due to the tremendous development and rapid growth of the ceramic construction industry in Egypt, solid wastes are expected to increase significantly. Therefore, efforts have been made to safely dispose these wastes and reuse them again as precious, fired, durable raw materials manufactured from natural resources, so valuable that they are sustainably utilized as the prices of the raw materials grow expensive. Therefore, the European Directives List of Wastes (European Waste Code 10.12.12,) [23, 24] does not consider ceramic tile wastes hazardous.

The waste that is utilized through this present work is the polishing powder that results from polishing the surface of the highest quality of ceramic tile of 0.5% water absorption and the 0.5-3% non glazed type as classified by both ISO and Egyptian standards [25, 26], commercially known as porcelain floor tiles and produced by Egyptian companies at a relatively high temperature. Utilization of this valuable fired, sound quality kaolin waste, was mainly in construction

industries. The development of both roughness and gloss with polishing time is well described by quantitative empirical models involving a simple exponential function [27]. Steiner, et al [28] utilized this waste to be added to cement mortars. Andreola et al. [24] mixed the "as received" ceramic sludge containing the polishing powder waste from two Italian factories with packaging glass cullet to obtain glass ceramics for ceramic wall or floor tiles. The sintering treatment at temperatures was in the order of 1000°C. The final products showed low porosity values, comparable water absorption, linear shrinkage and higher flexural strength values than the minimum needed by ISO 13006 [25] for commercial tiles. It was also utilized to produce paving blocks [29]. The consequences show that it is achievable to replace 30% of total fines or 20% of cement with polishing waste of ceramic tiles and create pavement blocks proper for use in heavy vehicle traffic. Wang et al. [30] utilized ceramic tile polishing waste, which is found in large amounts in China. This trash was effectively used as the major raw material in the production of foam ceramic. As a foaming agent, SiC (1% wt.) was added to the best composition. Sodium phosphate (as 2-3%wt) was added as a foam stabilizer to produce a foam ceramic with a superior structure. De Sousa et al. [31] made use of porcelain tiles polishing residues as a component of a mixture of a glassy phase, with water, organic substances, and abrasive particles, mainly SiC, found in the sludge. Results showed feasibility of producing cellular ceramics from this waste. Finally, recycling of the polishing waste of porcelain tiles in the same industry was investigated by Ke et al. [32].

Novelty proposed by the authors aims to assess the probability of obtaining a material appropriate for use as a floor covering tile buildings. In addition, this work aims to prepare green rubber composites that are environmentally beneficial for usage in commercial rubber products by replacing kaolin as one of the conventional fillers in the rubber industry with fired porcelain tiles polishing waste. This work leads to an evaluation of the mechanical and electrical properties of the prepared composites in addition to studying the thermal stability and surface morphological properties of the prepared composites.

## 2. Materials and techniques

### 2.1. Materials

Styrene/butadiene rubber (SBR) was provided by El-Nasr Company for Rubber Products, Egypt. Chemicals of commercial-grade such as stearic acid and zinc oxide (ZnO) as activators, paraffin oil, N-Cyclohexyl-2-benzothiazole sulphenamide (CBS), Tetramethylthiuram Disulfide (TMTD), and elemental sulfur were used without any further purification. 2,2,4-trimethyl-1,2-dihydroquinoline (TMQ) was used as an antioxidant of commercial grade type. Kaolin filler was obtained from Transport and Engineering Company, Alexandria, Egypt. Porcelain tile polishing waste (PTW) was obtained from an Egyptian company factory for ceramics production from Egyptian raw materials. It results due to surface polishing of the highest quality of the ceramic tile (non glazed, 0.5% water absorption and the 0.5-3%) [25,26] These tiles are self vitrified and fired at 1200 °C and are commercially known as porcelain floor tiles. It is extracted as slurry that must be dried to get this very fine powder, where in most cases, the water must be recycled to the factory process.

**Table 1: Formulation of SBR/PTW composites**

Ingredients, phr	Samples composition				
	E1	E2	E3	E4	E5
SBR	100	100	100	100	100
Kaolin	40	30	20	10	0
PTW	0	10	20	30	40
ZnO	4	4	4	4	4
Stearic acid	2	2	2	2	2
Paraffin oil	3	3	3	3	3
TMTD	1	1	1	1	1
CBS	0.8	0.8	0.8	0.8	0.8
TMQ	1	1	1	1	1

### 2.2. Assessment of the porcelain tiles waste (PTW)

Ceramic Porcelain tiles polishing waste fine powder, as received, was analyzed by X-ray fluorescence technique (XRF). Chemical analysis was carried out using Axios (PW4400) WD-XRF Sequential Spectrometer (Panalytical, Netherlands), using (Rubidium) Rb  $\alpha$  radiation tube at 50 kV and 50 mA. The powder X-ray diffractometry analysis was carried out for the waste to detect its mineralogical composition using the XRD apparatus X'Pert Pro

PW3040/60 (PANalytical) diffractometer equipped with monochromatic Rb- $\alpha$  radiation source. The test was run at 40 kV and 30 Ma. A continuous mode was used for collecting data in the  $2\theta$  range from  $3^\circ$  to  $30^\circ$  at a scanning speed of  $2^\circ/\text{min}$ . The acquired data were identified using X'Pert high score software works with a PDF-2 database. The waste fineness was considered through the Laser Scattering Particle Size Distribution Analyzer apparatus (Horiba LA950), based on volume distribution measurements.

### 2.3. Preparation and characterization of SBR composites

A laboratory two-roll mill was used to mix SBR with other used additives, and the formulations details were illustrated in Table 1. The rheological properties of SBR composites were evaluated using a Moving die rheometer (MDR 2000). According to ASTM D412 and by using an electronic Zwick tensile testing machine (model Z010, Germany) the mechanical properties of vulcanizates rubber which include tensile strength and elongation at break were performed. Hardness shore A was measured by a Zwick Roell durometer machine from (Germany). Furthermore, thermo-oxidative aging of the vulcanizates was performed according to ASTM: D 572-04, 2010, at a temperature of  $90^\circ\text{C}$  for 7 days.

The equilibrium swelling for SBR composites in toluene (Q%) was assessed and calculated according to (ASTM: D471- 06). Crosslinking density was measured and calculated according to the Flory-Rehner relation equation [16].

### 2.4. Thermal analysis

TGA was conveyed by using TGA/DSC 3+ (Mettler-Toledo Inc., USA), under nitrogen flow from 30 to  $600^\circ\text{C}$  with a heating amount of  $10^\circ\text{C}/\text{min}$ .

### 2.5. Phase morphology of SBR composites

The morphology of the composites was monitored by SEM, (JSM 6360LV, JEOL/Noran).

### 2.6. Dielectric measurements

The permittivity  $\epsilon'$  and the dielectric loss  $\epsilon''$  in addition to the electrical conductivity  $\sigma$  were performed by using Novo control Alpha Analyzer (GmbH concept 40,  $\tan\delta > 10^{-4}$ ). The measurements frequency range was from  $10^{-1}$  Hz to  $10^7$  Hz. The measurement cell was two gold parallel plates capacitor with a diameter of 10 mm. This technique can search molecular alternatives and charge progress in broad frequency range.

### 3. Results and discussion

#### 3.1. Characterization of porcelain tiles polishing waste powder (PTW)

Table 2 shows the chemical composition of the ceramic porcelain tiles polishing waste powder (PTW). Comparing this result with the Italian sludge used by Andreola et al. [24], the Egyptian waste used in this work is of higher quality, as it contains higher Magnesia and is not polluted by zirconia. The XRF of raw kaolin in previous literature [33] shows that the percentage of silica was 45.26%, followed by the percentage of aluminium oxide, which was 38.71%, and it contained small percentages of different oxides. The results of XRF proved that the chemical composition of porcelain tile (PTW) waste is more affluent in silica but poorer in alumina if compared with raw commercial kaolin. Being fired at a high temperature and including both Quartz and Spinel, as will be shown later, makes it possible to study the possibility of substituting commercial kaolin with this waste in styrene butadiene rubber with an evaluation of the mechanical and electrical properties of these compounds.

**Table 2: The chemical composition of porcelain tiles polishing waste (PTW)**

Main Constituents	Wt%
SiO <sub>2</sub>	64.30
TiO <sub>2</sub>	0.60
Al <sub>2</sub> O <sub>3</sub>	15.60
Fe <sub>2</sub> O <sub>3</sub>	0.71
MgO	7.04
CaO	0.97
K <sub>2</sub> O	0.80
Na <sub>2</sub> O	2.34
P <sub>2</sub> O <sub>5</sub>	0.42
SO <sub>3</sub>	0.53
Cl	0.66
Cr <sub>2</sub> O <sub>3</sub>	0.03
BaO	0.21
L.O.I	5.66

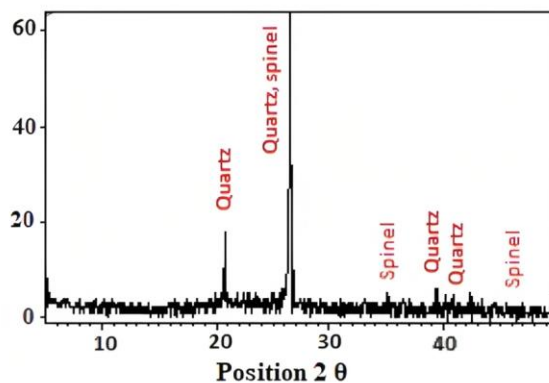


**Fig.1: XRD pattern of porcelain tiles polishing waste**

The pattern in Fig.1 shows that this fired waste of high quality kaolin contains both Quartz (SiO<sub>2</sub>) (Reference code 01-083-0539) and Spinel (Mg Al<sub>2</sub> O<sub>4</sub>) (Reference code 00-003-0901). This result agrees with the chemical composition shown in table 2 where silica, alumina and magnesium oxide form the highest weight percentages successfully.

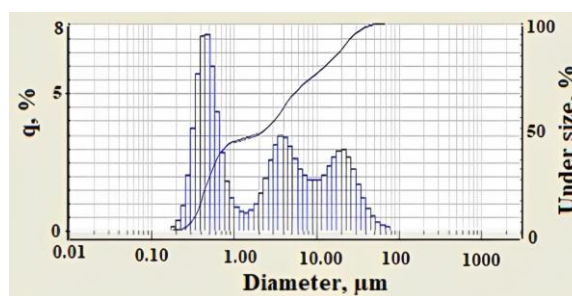


**Fig. 2: Particle size distribution of porcelain tiles polishing waste**

Fig.2 shows the particle size distribution of the waste powder as received. The pattern showed 3 peaks of the normal distribution, which has no significant differences as long as the powder is very fine. The particle size distribution analysis is explained by the direct and calculated parameters of the analyzer, as shown in Table 3. As will be shown later, the fineness of the waste was an influential factor for future results.

**Table 3: Particle size distribution of the porcelain tiles polishing waste**

Item	PTW
Mean size, $\mu\text{m}$	7.222
Median size, $\mu\text{m}$	2.626
Mode size, $\mu\text{m}$	0.47
Diameter on cumulative of 10%, $\mu\text{m}$	0.364
Diameter on cumulative of 90%, $\mu\text{m}$	22.445
Size range, $\mu\text{m}$	0.172 to 77.333

### 3.2. Characterization of SBR/PTW composites

#### 3.2.1. Rheological characteristics of SBR/PTW composites

Figure 3(a-c) shows the cure curves for styrene butadiene rubber composites. From figure (3a,b), it is clear that the value of minimum torque ( $M_L$ ) and maximum torque ( $M_H$ ) of SBR composites grew steadily as PTW waste weight ratio was increased, which is explained by the fact that SBR composites were stiffer as PTW waste powder and conventional kaolin were added as fillers. In other words, the increase in the  $M_H$  value of SBR filled with ceramic waste was closely correlated with the decrease in SBR chains' mobility brought on by adding fillers. The increase in torque values may be due to good interactions between SBR and waste (PTW) filler surfaces [34]. More significantly, for rubber composites, the torque difference, the difference between the maximum ( $M_H$ ) and minimum ( $M_L$ ) torque was considered as indirect indicator of the cross-link density [34, 35]. As shown in Figure 3c, the torque difference value increased continuously with increasing PTW waste weight ratio for SBR composites. Incorporation PTW waste filler has accelerated vulcanization process with a significant decline in scorch time  $t_{s2}$  and optimum curing time  $T_{c90}$  as shown in figure 4. This decrease may be due to the interfacial adhesion between filler and matrix as a result of the fines of PTW particles.

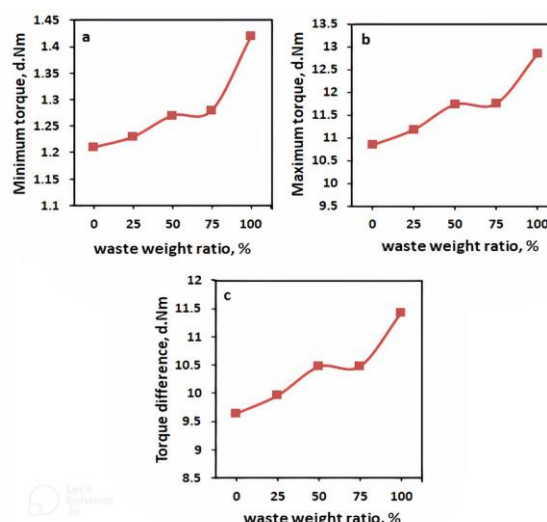


**Fig. 3: Relationship between torques versus PTW waste weight ratio for SBR composite**

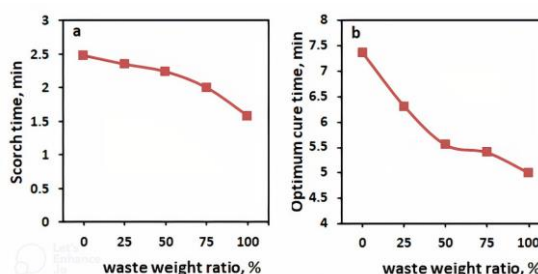


**Fig.4: Scorch time and optimum cure time in min versus PTW waste weight ratio for SBR composites**

**a: Scorch time b: Optimum cure time, min**

#### 3.2.2. Mechanical properties of SBR/PTW composites

Figure 5(a-b) illustrates the tensile strength and elongation at break of SBR filled with commercial kaolin and substituted ratios of PTW waste powder. From this figure, it can be seen that the incorporation of ceramic waste has positive effect on the tensile strength of SBR composites, where the tensile strength increased from 8.7 MPa for SBR filled with pure kaolin to 9.35, 9.5, 9.8 and 10.25MPa for SBR filled with substitution ratios of kaolin and porcelain tile grinding waste (PTW) (75:25), (50:50), (25: 75) and (0: 100) respectively. The highest tensile strength was achieved by SBR filled with 100 % PTW weight ratio. The increment in tensile strength may be due to the interfacial bond between SBR and waste filler resulting from the good scattering of the fine particles in the rubber composites, most probably because of the fineness and stability due to high firing temperature of the waste. In contrast, elongation at

break decreases with increasing substitution ratio of PTW waste. The value of elongation at break for SBR filled with pure kaolin was 612 % and declined to 579 % for SBR filled with PTW powder waste. This decline may be due to the increment of composite stiffness with increasing the waste filler substitution ratio [14]. Figure 5c illustrates the relation between hardness shore A versus waste filler weight ratio. This figure shows that the hardness shore A increased gradually with increasing the substitution ratio of traditional kaolin with PTW powder waste. Hardness shore A increased from 66 for SBR filled with kaolin to reach the highest value for SBR filled with 100% PTW which was 75.

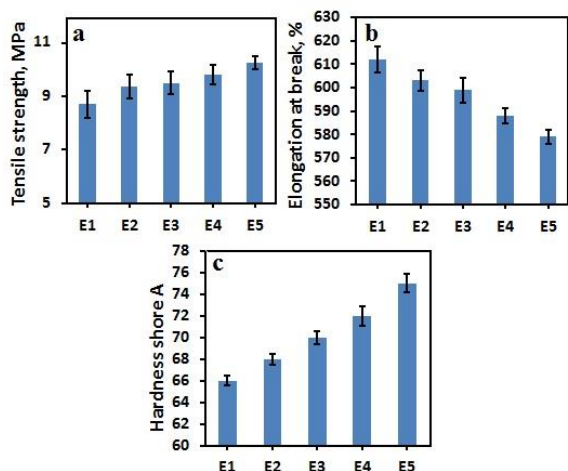


**Fig.5: Mechanical parameters for SBR/PTW composites**

### 3.2.3. Thermo-oxidative aging of SBR/PTW composites

The thermo-oxidative aging is the most crucial test to determine whether products can endure weather conditions since weather elements impact the quality of the end products [36]. The effect of substituting traditional kaolin with ceramic waste on the thermal aging resistance of SBR composites was assessed through the variations in the retained values of tensile and elongation at break. Figure (6a,b) points up the reserved tensile and elongation at break amount through 7 days at 90°C for SBR/Kaolin and SBR filled with different substituted ratios from ceramic waste. This figure reflects the decrease in the tensile retained value with increasing aging time. The highest tensile strength retained values were achieved by SBR filled with 100 % PTW which was 90.24% followed by SBR filled with 75% PTW waste filler. While the lowest tensile strength retained value was

achieved by SBR filled with kaolin which was 85.06%. The retained values of elongation at break for prepared composites had the exact behavior of the retained values of tensile strength where the highest retained value was achieved by SBR filled with 100% PTW which was 86.8% and the lowest value achieved by SBR/100% kaolin which was 80.01%.

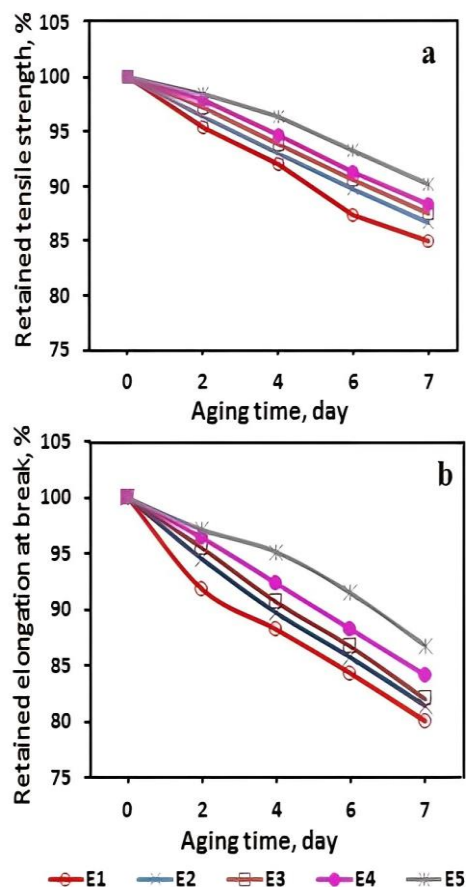


**Fig. 6: Retained mechanical properties of SBR composites after aging 7 days at 90°C**

### 3.2.4. Swelling and cross-link density of SBR/PTW composites

Cross-link density is a notable factor directly related to the vulcanization and mechanical properties of filled composite materials. The discrepancy in the crosslink density of SBR compounds, including PTW waste and swelling behavior is displayed in Table 4. It is notable from this table that the incorporation of ceramic waste positively affected the swelling behavior of prepared samples. On the other hand, the solvent uptake ratio for SBR composites decreased with increasing the PTW waste weight ratio from 268.34% for SBR filled with traditional kaolin to

246.57 % for SBR filled with waste ceramic. As the waste filler quantity in SBR composites increased, the cross-link density increased consistently. Actually, as filler loading increased, the molecular mobility of the SBR chains gradually decreased, making it harder for toluene to pass through the SBR matrix [37]. In addition, the crosslink density increased with increasing the PTW waste weight ratio from 1.22 for SBR filled with kaolin to 1.441 for SBR filled with PTW waste filler. These results are in line with the results of the rheological properties. Sae-oui et al. [38] have previously observed that including basic filler increases the cross-link density of rubber composites.

**Table 4: Equilibrium swelling and crosslink density for SBR composites**

Samples	Equilibrium swelling, Q <sub>m</sub>	Crosslinking density, $\nu$ , mol/cm <sup>3</sup> x10 <sup>-4</sup>
E1	268.34	1.221
E2	266.67	1.236
E3	266.29	1.239
E4	260.75	1.291
E5	246.57	1.441

### 3.2.5. Thermal analysis of SBR/PTW composites

Figure 7 illustrates the TGA graphs of SBR filled with kaolin and PTW ceramic waste. Also, Table 5 lists the thermal characteristics of SBR composites. It is clear that when PTW waste was added to the SBR matrix, the value of T<sub>i</sub> slightly increased. However, when compared to the SBR filled with kaolin, the SBR filled with 100% PTW waste exhibited a considerable increase in the value of T<sub>i</sub>. Additionally, T<sub>20%</sub> and T<sub>50%</sub> values were significantly higher in the SBR/100% porcelain ceramic waste system than in the system filled with kaolin, indicating that the thermal stability of SBR composites was successfully enhanced by the supplement of porcelain ceramic waste as filler. This result is expected due to the stability of the fired waste other than including higher Silica and Spinel minerals (Fig.1).

Also, residue mass increased with adding porcelain ceramic waste, where the highest mass residue was achieved for SBR filled with 50% PTW waste, which was 28.5% followed by SBR filled with 100% PTW. This confirms the thermal stability of SBR composites.

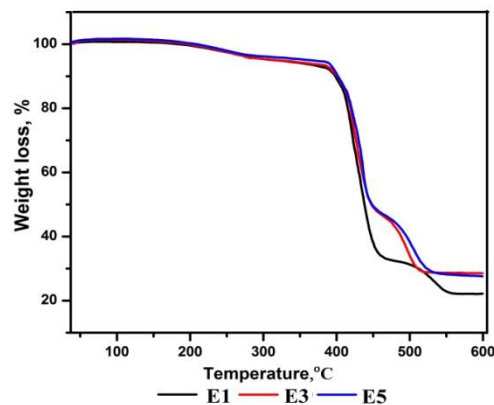


**Fig. 7: TGA curves for SBR filled with kaolin and substituted ratios from PTW waste**

**Table 5: Thermal degradation of SBR /PTW composites**

Samples code	Tem (°C)			Residue wt% at 600°C
	T <sub>i</sub>	T <sub>20%</sub>	T <sub>50%</sub>	
E1	377	415	438	22
E3	383	412	437	28.5
E5	387	419	448	27

T<sub>i</sub>: Initial degradation temperature, T<sub>20%</sub>: Temperature at 20% weight loss, T<sub>50%</sub>: Temperature at 50% weight loss

### 3.2.6. Morphology of SBR/PTW

SEM images of SBR filled with 100% kaolin, SBR/kaolin: PTW (50:50) and SBR filled with 100% PTW composites were depicted in Figure 8. This figure shows that the filler dispersion was better in the case of SBR filled with 100% PTW (E5). Also, it becomes apparent that the best fillers dispersion exhibits the sample filled only with 100% PTW. With increasing the content of kaolin and decreasing the PTW content, the filler dispersion degree gradually decreases, as shown in E3. Simultaneously, the surface of filler agglomerates and aggregates becomes larger in the case of SBR filled with 100% kaolin as shown in (E1).

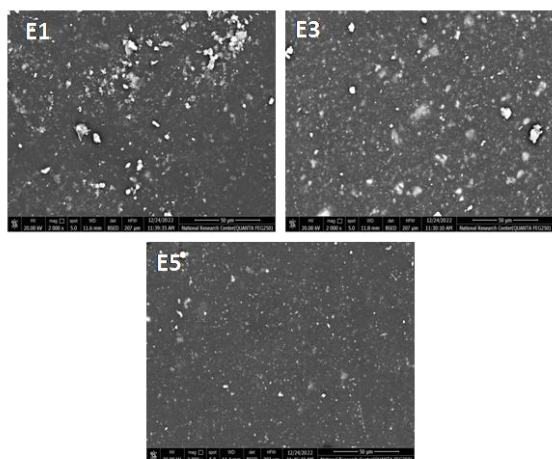


**Fig. 8:** Scanning electron microscope for SBR filled with kaolin and PTW waste

### 3.2.7. Dielectric measurements of SBR/PTW composites

The dielectric properties, including permittivity  $\epsilon'$ , dielectric loss  $\epsilon''$  and loss tangent  $\tan \delta$  were deliberated over the frequency range 0.1 to  $10^7$  Hz at room temperature. ( $\sim 25^\circ\text{C}$ ) the obtained data were presented in Figure (9). The permittivity  $\epsilon'$  was found to enlarge by increasing the waste weight ratio. This increase could be explained according to Maxwell Wagner's effect due to the charge accumulation in the interfaces between the filler and rubber matrix. In addition, according to the micro capacitor model, the relatively high conductivity of filler is separated by insulator SBR that form micro capacitor structure from SBR as a dielectric material and filler as electrode [39, 40].

Values of  $\epsilon'$  were found to decrease dramatically by rising the frequency, which preserve to the enhancement in the polarization courses e. g. dipolar and interfacial polarization [39-42]. Low-frequency dipoles can overcome internal resistance and align their orientation to the applied electric field. However, due to internal resistance, a few dipoles cannot keep up with the change in field direction as the field frequency increases. As a result, relaxation occurs, lowering the dielectric constant at high frequencies.

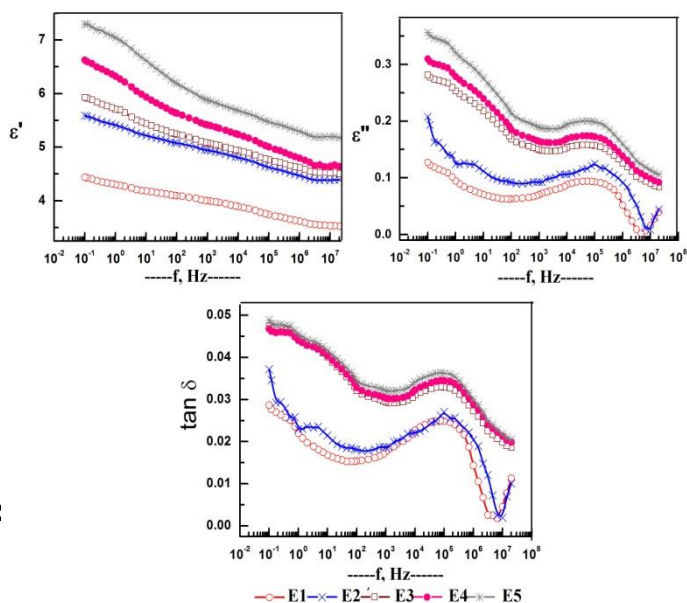


**Fig. 9:** The permittivity  $\epsilon'$ , dielectric loss  $\epsilon''$  and loss tangent  $\tan \delta$  for SBR loaded with PTW versus the applied frequency  $f$ , at room temperature  $\sim 25^\circ\text{C}$

Both  $\epsilon''$  and  $\tan \delta$  values depicted in Figure (9) reflect very complicated curves that indicate more than one relaxation process. The most identified one at the high frequency range was found to shift slightly towards the lower frequency by increasing waste percentage in the hybrid filler, indicating an interaction between filler and polymer matrix. Anyhow, both values increase by increasing waste percentage. However, this increase is still in good order, which makes the end composite suitable for insulation purposes, which appeared by plotting  $\epsilon'$ , and  $\epsilon''$  versus waste content at a fixed frequency  $f = 100$  Hz in Figure (10).

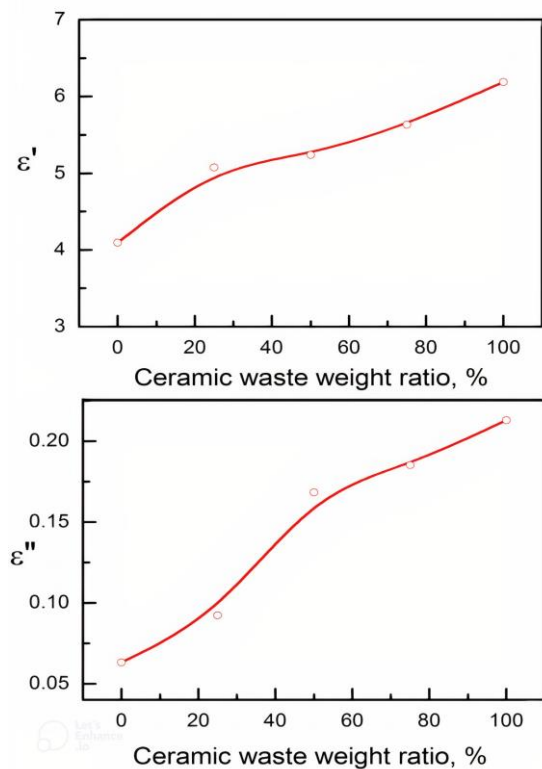


**Fig. 10:** The permittivity  $\epsilon'$ , dielectric loss  $\epsilon''$  versus the waste content at fixed frequency  $f=100\text{Hz}$ .

The  $\sigma$  values were computed from the measured resistance, and the data obtained was shown graphically in Figure (11) versus waste content. This figure shows that  $\sigma$  values lie in the order of  $10^{-15}\text{S/cm}$  although  $\sigma$  values increase by increasing waste content.

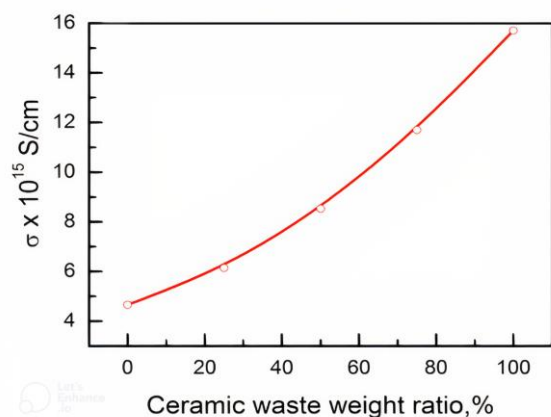


**Fig. 11:** The dc electrical conductivity  $\sigma$ , versus the waste weight ratio

This finding recommends these composites be used for insulating purposes. In addition, the kaolin could be replaced safely by PTW waste as the dielectric properties improve as the waste weight ratio increases.

### Conclusion

XRF analysis proved that the chemical composition of porcelain tiles polishing waste powder (PTW) is richer in silica but poorer in alumina than raw commercial kaolin. Also, XRD illustrates that this fired waste of high quality kaolin contains both Quartz ( $\text{SiO}_2$ ) and Spinel ( $\text{Mg Al}_2 \text{O}_4$ ). In addition, particle size distribution illustrates that the waste powder is very fine. Therefore, the replacement of commercial kaolin with PTW was studied as green and economical filler for styrene butadiene rubber (SBR). The inclusion of PTW in SBR composite with the sulphur cure system created in this study was an adequate substitute for conventional kaolin as reinforcing filler in the rubber industry. The mechanical measurements conclude that incorporating PTW as a filler develops both tensile strength and shore A hardness. In contrast, decrease in the elongation at break with increasing the waste weight ratio was detected. Furthermore, the electrical investigations revealed that the values of  $\epsilon'$  are found to enhance by increasing PTW weight ratio. The values of  $\sigma$  were in the order of  $10^{-15}\text{S/cm}$  even by increasing waste weight ratio that reflect the improvement in the insulation properties of SBR composites.

### Conflict of interest

The authors declare that they have no conflict of interest

### References

1. Skalková P., Počarovský P., Čakánek P., Pajtašová M. and Benčíková E., Using of TPE waste in blends with natural rubber, in: 6th International conference on polymeric materials in automotive, 22nd Slovak rubber conference, Book of proceedings, 234–237, ISBN 978-80-970923-7-5, (2015).
2. Skalková P. and Labaj I., Study of mechanical properties of NR/Biopolymer blends, Metallurgical journal, 67(3), 60–64, (2014).
3. Wei H., Guo L., Zheng J., Huang G. and Li G., Effect of nanosilica-based immobile antioxidant on thermal oxidative degradation of SBR. RSC Advances 5, 62788–627965, (2015).

4. Rozik, N.N., Abd-El Messieh, S.L., Rabie, A.M., Shafik, E.S. and Younan, A.F., Mechanical and electrical properties of SBR composite filled with modified magnesium hydroxide by functionalized ionic liquid, *Kautschuk Gummi Kunststoffe*, 71 (5), 49-55, (2018).
5. Rezig N., Bellahcene T., Aberkane M. and Abdelaziz M. N., Thermo-oxidative ageing of a SBR rubber: effects on mechanical and chemical properties. *Journal of Polymer Research* 27(339), 1-13,(2020).
6. Roy K., Debnath S. C., Bansod N. D., Pongwisuthiruchte A., Wasanapiarnpong T. and Potiyaraj P., Possible use of gypsum waste from ceramics industry as semi-reinforcing filler in epoxidized natural rubber composites. *Journal of Material Cycles and Waste Management*, 22:285–294,(2020).
7. Sheikh S. H., A study of the effects of kaolin, solid filler on the processing, mechanical, and dynamic properties of some industrial rubbers cured with novel sulphur cure system. PhD thesis, Loughborough University,(2017).
8. Dewi R., Agusnar H., Alfian, Z. and Tamrin, Characterization of technical kaolin using XRF, SEM, XRD, FTIR and its potentials as industrial raw materials. *Journal of Physics: Conf. Series*, 1116, 042010, (2018).
9. Zhang Q., Zhang Y. and Wang Y., Mechanical and thermal properties of kaolin/natural rubber nano-composites prepared by the conventional two-roll mill method, *Applied Mechanics and Materials*,164, 142-145, (2012)
10. Shafik E. S., Tharwat C. and Abd-El-Messieh S. L., Utilization study on red brick waste as novel reinforcing and economical filler for acrylonitrile butadiene rubber composite. *Clean Technologies and Environmental Policy*, 1-11, <https://doi.org/10.1007/s10098-022-02457-0>, (2022).
11. Rozik N. N., Yakoob J., Saad E. and Abdel-Messeh S. L., Mechanical and electrical Properties of Acrylonitrile Butadiene Rubber filled with Waste Carbon. *KautschukGummiKunststoffe KGK*,70(4), 30-35, (2017).
12. Abd El-Aziz M. E., ShafikE. S., TawficM. L. andMorsiS. M. M.,Biochar from waste agriculture as reinforcement filer for styrene/butadiene rubber. *Polymer Composites*, 43 (3), 1295-1304, (2022)
13. Saied M., Reffae A., Hamieda S., Abd-El-Messieh S. L. and Shafik E. S. Eco-friendly polymer composite films based on waste polyvinyl chloride/sunflower seed cake for antimicrobial and antistatic applications. *Pigment & Resin Technology*, Doi. [https://doi.org/10.1108/PRT-10-2021-0126\(2022\)](https://doi.org/10.1108/PRT-10-2021-0126(2022)).
14. Saleem M., Butt M.S., Maqbool A., Umer M.A., Shahid M., Javaid F., Malik R.A., Jabbar H., Waseem H.M., Khalil L.D., Hwan M., Kim B. K., Koo and Jeong S.J., Percolation phenomena of dielectric permittivity of a microwave-sintered BaTiO<sub>3</sub>-Ag nanocomposite for high energy capacitor, *Journal of Alloys and Compounds*, 822, 153525, <https://doi.org/10.1016/j.jallcom.2019.153525>, (2020).
15. Li L., Zhou B., Ye J., Wu W., Wen F., Xie Y., Bass P., Xu Z., Wang L., Wang G. and Zhang Z., Enhanced dielectric and energy-storage performance of nanocomposites using interface-modified anti-ferroelectric fillers, *Journal of Alloys and Compounds*, 831,154770, <https://doi.org/10.1016/j.jallcom.2020.154770>, (2020).
16. Ram F., Kaviraj P., Pramanik R., Krishnan A., Shanmuganathan K. and Arockiarajan A., PVDF/BaTiO<sub>3</sub> films with nanocellulose impregnation: Investigation of structural, morphological and mechanical properties, *Journal of Alloys and Compounds*, 823, 153701, <https://doi.org/10.1016/j.jallcom.2020.153701>, (2020).
17. Luo S.B., Shen Y.B., Yu S.H., Wan Y.J., Liao W.H., Sun R. and Wong C.P., Construction of a 3D-BaTiO<sub>3</sub> network leading to significantly enhanced dielectric permittivity and energy storage density of polymer composites, *Energy & Environmental Science*, 10 137–144, <https://doi.org/10.1039/c6ee03190k>,(2017).
18. Guo C. and Fuji M., Effect of silicone coupling agent on dielectric properties of barium titanate/silicone elastomer composites, *Advanced Powder Technology*, 27, 1162–1172, <https://doi.org/10.1016/j.appt.2016.03.028>,(2016).
19. Xie L., Huang X., Huang Y., Yang K. and Jiang P., Core@Double-shell structured BaTiO<sub>3</sub>-

- polymer nanocomposites with high dielectric constant and low dielectric loss for energy storage application, *The Journal of Physical Chemistry C*, 117, 22525–22537, <https://doi.org/10.1021/jp407340n>, (2013)
20. Uyor U.O., Popoola A.P.I., Popoola O.M. and Aigbodion, V.S., Thermal, mechanical and dielectric properties of functionalized sandwich BN-BaTiO<sub>3</sub>-BN/polypropylene nanocomposites, *Journal of Alloys and Compounds*, 894 162405, <https://doi.org/10.1016/j.jallcom.2021.162405>, (2022)
  21. Koner S., Deshmukh P., Ahlawat A., Karnal A.K. and Satapathy S., Studies on structural, dielectric, impedance spectroscopy and magneto-dielectric properties of La<sub>0.7</sub>Ba<sub>0.3</sub>MnO<sub>3</sub>/P(VDF-TrFE) multiferroic (0–3) nanocomposite films, *Journal of Alloys and Compounds*, 868, 159104, <https://doi.org/10.1016/j.jallcom.2021.159104>, (2021).
  22. Wu Z., Zhou H., Guo Q., Liu Z., Gong L., Zhang Q., Zhong G., Li Z. and Chen Y., Enhanced dielectric properties in polyimide nanocomposites containing barium titanate@polydopamine core-shell nanoparticles, *Journal of Alloys and Compounds*, 845 156171, <https://doi.org/10.1016/j.jallcom.2020.156171>, (2020).
  23. Juan A., Medina C., Moran J.M., Guerra M.I., Aguado P.J., Isabel M., Sanchez de Rojas M.I., Frias M. and Rodriguez O., *Ceramic Materials, Chapter (10): Reuse of Ceramic Wastes in Construction*, 1st ed., In Tech, ISBN: 978-953-307-145-9, 197 (2010).
  24. Andreola F., Lancellotti I., Pozzi P. and Barbieri L., Eco-compatible Construction Materials Containing Ceramic Sludge and Packaging Glass Cullet, *Applied Sciences* 11(3545), 1-17, (2021).
  25. ISO 13006/2018, *Ceramic tiles –Definitions, classification, characteristics and marking*, International Organization for Standardization ISO
  26. ES 3168/2015, *Ceramic Tiles, parts 1,2,3 ( under development)*, Egyptian Organization for Standardization and Quality (EOS), Cairo, Egypt
  27. Hutchings I. M., Xu Y., Sa' Nchez E., Iba' N' Ez M. J. and Quereda M. F., Development of surface finish during the polishing of porcelain ceramic Tiles. *Journal Of Materials Science*, 40, 37 – 42, (2005)
  28. Steiner L. R., Bernardin A. M. and Pelisser F., Effectiveness of ceramic tile polishing residues as supplementary cementitious materials for cement mortars, *Sustainable Materials and Technologies*, 4, 30-35, (2015), <http://dx.doi.org/10.1016/j.susmat.2015.05.001>
  29. Penteado C. S. G., Viviani de Carvalho E. and Lintz R. C. C., Reusing ceramic tile polishing waste in paving block manufacture, *Journal of cleaner production*, 112(1), (2016).
  30. Wang H., Chen Z., Liu L., Wang X., Ji R., Synthesis of a foam ceramic based on ceramic tile polishing waste using SiC as foaming agent, *Ceramics international*, 44(9), (2018).
  31. De Sousa I. V., Nieves L. J. J., Dal-Bó A. G. and Bernardin A. M., Valorization of porcelain tile polishing residue in the production of cellular ceramics, *Cleaner engineering and technology*, 6, 100831, (2022).
  32. Ke S., Wang Y., Pan Z., Ning C. and Zheng S. Recycling of polished tile waste as a main raw material; in porcelain tiles, *Journal of cleaner production*, 115, 238-244, (2016).
  33. El-Sabbagh S. H., and Ahmed N.M. Enhancement of styrene-butadiene rubber composites using kaolin covered with metal oxide pigments. *Pigment & Resin Technology*, 44(2), 57–73, (2015).
  34. Intiya W., Thepsuwan U., Sirisinha C. and Sae-Oui P., Possible use of sludge ash as filler in natural rubber. *Journal of Material Cycles and Waste Management*, 19, 774–78, (2017).
  35. Ismail H. and Shaari S. M., Curing characteristics, tensile properties and morphology of palm ash/halloysite nanotubes/ethylene-propylene-diene monomer (EPDM) hybrid composites. *Polymer Testing*, 29, 872–878, (2010).
  36. Hassan A.M. A., Shafik E. S., Hussein A. I., Derbala H. A., Elziaty A.K. and Elsayed G.A., Synthesis of 2-alkylbenzimidazole moiety as a novel antioxidant and its effect on physico-mechanical and electrical properties of acrylonitrile butadiene rubber, *Egyptian Journal of Chemistry*, 63(6), 2235-2248, (2020).
  37. Roy K., Debnath S. C., Bansod N. D., Pongwisuthiruchte A., Wasanapiarnpong T. and Potiyaraj P., Possible use of gypsum waste from ceramics industry as semi-reinforcing filler in epoxidized natural rubber composites. *Journal*

- of Material Cycles and Waste Management, 22, 285–294, (2020).
38. Sae-oui P., Sirisinha C. and Thaptong P Utilization of limestonedust waste as filler in natural rubber. Journal of Material Cycles and Waste Management,11, 166–171, (2009).
  39. Zenga Y., Xionga C., Lib W., Raoa S., Dua G., Fanc Z. and Chena N., Significantly improved dielectric and mechanical performance of Ti3C2Tx MXene/silicone rubber nanocomposites, Journal of Alloys and Compounds 905,164172,(2022).
  40. Shafik E.S., Ward A. A. and Younan A.F., Essential oils as multifunctional additives in biodegradable linear low density polyethylene/starch blends, Pigment & Resin Technology , 51(2), 194-203, (2022).
  41. Shafik E. S., Rozik N. N., Younan A.F., and Abd El-Messieh S.L., Novel plasticizer for acrylonitrile butadiene rubber (NBR) and its effect on physico-mechanical and electrical properties of the vulcanizates, Bulletin of Materials Science, 43(1), 1-8, (2020).
  42. Abd El-Messieh S. L., Younan A. F., Shafik E. S. and Rozik N. N., Ionic conductivity and mechanical properties of ionic liquids incorporated PMMA based polymer electrolytes. Kautschuk Gummi Kunststoffe-KGK, 71 (3), 26-31, (2018).